Phylodynamic inference of contact network parameters through approximate Bayesian computation

Rosemary M. McCloskey and Art F.Y. Poon

February 1, 2016

Contents

List of Figures

List of Symbols

I number of nodes which are eventually infected.

N number of nodes in the network.

α preferential attachment power parameter in Barabási-Albert networks.

λ decay factor meta-parameter for tree kernel.

σ radial basis function variance meta-parameter for tree kernel.

m number of edges added per vertex when constructing a Barabási-Albert network.

List of Abbreviations

ABC approximate Bayesian computation.

BA Barabási-Albert.

ER Erdős-Rényi.

MCMC Markov chain Monte Carlo.

ML maximum likelihood.

nLTT normalized lineages-through-time.

PCA principal components analysis.

pdf probability density function.

SI susceptible-infected.

SVM support vector machine.

WS Watts-Strogatz.

Chapter 1

Introduction

1.1 Phylogenetics and phylodynamics

1.1.1 Phylogenetic trees

In evolutionary biology, a *phylogeny*, or *phylogenetic tree*, is a graphical representation of the the evolutionary relationships among a group of organisms or species (generally, *taxa*) (Haeckel 1866). The *tips* of a phylogeny, that is, the nodes without any descendants, correspond to *extant*, or observed, taxa, while the *internal nodes* correspond to their common ancestors. The edges or *branches* of the phylogeny connect ancestors to their descendants. Phylogenies may have a *root*, which is a node with no descendants distinguished as the most recent common ancestor of all the extant taxa (Harding 1971). When such a root exists, the tree is referred to as being *rooted*; otherwise, it is *unrooted*. The structural arrangement of nodes and edges in the tree is referred to as its *topology* (Cavalli-Sforza and Edwards 1967).

The branches of the tree may have associated lengths, representing either evolutionary distance or calendar time between ancestors and their descendants. The term "evolutionary distance" is used here imprecisely to mean any sort of quantitative measure of evolution, such as the number of differences between the DNA sequences of an ancestor its descendant, or the difference in average body mass or height. Particular examples of evolutionary distance, based on genetic data, will be discussed below in subsection 1.1.3. A phylogeny with branch lengths in calendar time units is often referred to as *time-scaled*. In a time-scaled phylogeny, the internal nodes can be mapped onto a timeline by using the tips of the tree, which usually map to the present day, as a reference point (Nee, Mooers, and Harvey 1992). The corresponding points on the timeline are called *branching times*, and the rate of their accumulation is referred to as the *branching rate*. Rooted trees whose tips are all the same distance from the root are called *ultrametric* trees (Buneman 1974). These

concepts are illustrated in Figure 1.1.1.

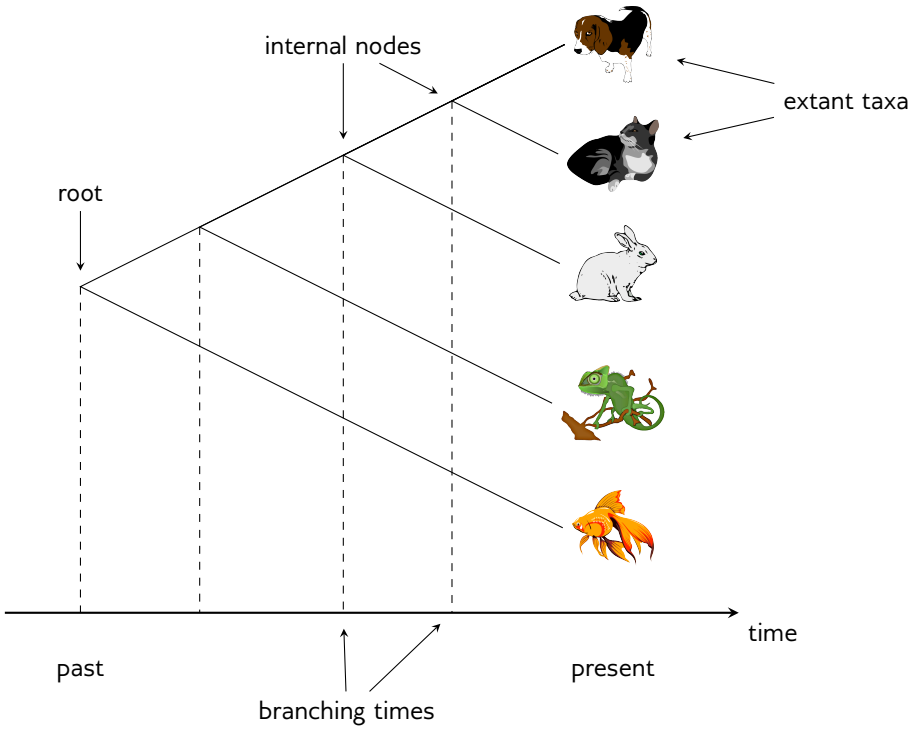

Figure 1.1: Illustration of a rooted, ultrametric, time-scaled phylogeny. The tips of the tree, which represent extant taxa, are placed at the present day on the time axis. Internal nodes, representing extinct common ancestors to the extant taxa, fall in the past. The topology of the tree indicates that cats and dogs are the most closely related pair of species, whereas fish is most distantly related to any other node in the tree.

1.1.2 Species trees and transmission trees

A *species tree* is a particular type of phylogeny in which the taxa are species, and the branching times correspond to historical speciation events. By speciation events, we mean times when two formerly interbreeding groups of organisms ceased to reproduce with each other. In general, we do not have access to the true tree relating a particular group of extant species, as this would usually imply certain knowledge of speciation events in the distant past. Therefore, all species trees considered by researchers are estimates, based on the genetic or phenotypic similarity of the extant taxa, the fossil record, or both. We discuss some of the challenges associated with this estimation in subsection 1.1.4 below. However, for the moment, we ignore these complications and consider what can be said about the true species tree.

Speciation often occurs by an *allopatric* process, where a sub-population of organisms is isolated from the original population by a geographic barrier (Coyne and Orr 2004). Over time, differing selection pressures on either side of the barrier, coupled with genetic drift,

cause the two populations to diverge genetically. This eventually results in two distinct species, which will appear as two subtrees or *clades* in their species tree if descendants of both survive to the present. Speciation is not necessarily allopatric: *sympatric* speciation refers to the emergence of a new species without any geographic barrier (Coyne and Orr 2004). Indeed, there is a whole continuum of possible speciation processes (Fitzpatrick, Fordyce, and Gavrilets 2008), ranging from completely allopatric to completely sympatric. However, at least for eukaryotic organisms, allopatric speciation is thought to be by far the most common type (Coyne and Orr 2004).

A different type of tree used in the study of pathogens is a *transmission tree*. In such trees, tips represent infected hosts, while internal nodes correspond to transmissions from one host to another. Transmission trees generally have branch lengths in units of calendar time, with a root corresponding to the index case, and branching times indicating times of transmission. The internal nodes may be labeled with the donor of the transmission pair, if this is known. The tips of the tree, rather than being fixed at the present day, are placed at the time at which the pathogen population of the individual was sampled. Consequently, the transmission tree may not be ultrametric, but may have tips located at varying distances from the root. Such trees are said to have *heterochronous* taxa or samples (Drummond et al. 2003), in contrast to the *isochronous* samples found in macro-organisms species trees. A transmission tree is illustrated in Figure 1.2.1 (A).

A priori, transmission trees and species trees have nothing to do with each other. One represents the evolutionary history of a group of organisms, the other traces the spread of a disease through a host population. However, when considering epidemics of RNA viruses, transmission trees and species trees are highly related. The viral population within a single host has often been referred to as a *quasispecies* (Domingo, Sheldon, and Perales 2012), and due to the fast evolutionary rate of these viruses, two hosts' viral populations are invariably genetically distinct. The transmission process is functionally identical to allopatric speciation, involving geographic isolation of a sub-population in a new host and subsequent genetic divergence. However, for the most part, it is not selection but rather host epidemiology which causes certain lineages to proliferate while driving others to extinction. A host who recovers, dies, or is isolated equates to an extinction in the transmission tree. On the other hand, dense populations in frequent contact often experience rapid epidemic growth, which causes similarly rapid accumulation of branching points in the tree.

The fact that these evolutionary (ie. speciation) and epidemiological processes occur on the same time scale for RNA viruses (Drummond et al. 2003) is the basis for the field of *phylodynamics* (Grenfell et al. 2004). The similarity between transmission and speciation means that it is possible to apply many of the tools and techniques developed for species trees to viral transmission trees, and interpret the results in the context of transmission rates and host epidemiology. As a basic example, the lineages-through-time plot (Nee,

Mooers, and Harvey 1992), which plots the historical speciation rate against time, can be used to quantify the incidence of new infections over the course of an epidemic (Holmes et al. 1995). In subsection 1.1.5 below, we review some of these methods in more detail, as well as several which have been developed specifically for viral phylodynamics, and discuss what these methods can tell us about host epidemiology.

Finally, we must note two important points. First, we have not yet considered the selection pressures operating within a single host, such as immune pressure, because these forces do not directly impact transmission trees unless they cause a host to recover or die. Second, we reiterate that both transmission trees and species trees are theoretical objects which are almost never known with certainty for real data. Indeed, the estimation of transmission trees is often problematic, and it is in such estimation that within-host forces play a role. Both of these issues are discussed further below in subsection 1.1.4, though we continue to ignore them in the next subsection.

1.1.3 Gene trees and viral phylogenies

A *gene tree* is another type of phylogeny which traces the evolutionary history of one or more sections of genetic material. Gene trees can be built from small parts of genes up to whole genomes, but for ease of exposition we will use only the word "gene". The tips of a gene tree represent the different *alleles*, or versions, of the gene found in the studied taxa. The branching points in a gene tree represent genetic divergence events - that is, the times when two distinct alleles first came into existence through mutation.

Gene trees are usually estimated using the nucleotide or amino acid sequences of the genes in question. Although there are methods for estimating gene trees using other types of molecular data, such as gene orders, we will focus on sequence-based methods here. As with species trees, it is not possible to know gene trees with certainty, only to estimate them. However, the problem of estimating gene trees directly from data is somewhat better defined than that of estimating species trees, because of the quantitative nature of the molecular data used to label the tips. In general, methods to estimate gene trees fall into three major categories: distance-based, maximum parsimony, and model-based (Nei and Kumar 2000). The first two categories are generally no longer used for phylogenetic inference, since model-based methods have been demonstrated to be almost universally more accurate. Therefore, we will review in detail only the last category.

Model-based methods include both maximum likelihood and Bayesian approaches. To use them, one must first define a parametric model of sequence evolution, here denoted M. For all possible trees T (with branch lengths) and choices of model parameters θ, the model must define a probability density function on observed sequence data D, denoted $f(D \mid T, \theta)$. This is also sometimes written $\Pr(D \mid T, \theta)$, even though it is a probability

density, not a probability. Maximum likelihood aims to find a particular tree and values for the model parameters which optimize the *likelihood function* $\mathcal{L}$ for the observed data,

$$\mathcal{L}(\theta, T \mid D) = f(D \mid T, \theta).$$

Bayesian methods, rather than trying to find point estimates for θ and T, aim to approximate the entire *posterior distribution* for the observed data,

$$f(T, \theta \mid D) = \frac{f(D \mid T, \theta) f(T, \theta)}{f(D)}.$$

Here, $f(T, \theta)$ denotes the prior distribution on T and θ, and $f(D)$ is the marginal density of the data (that is, the integral of the numerator over all values of T and θ).

A *viral phylogeny* is a particular kind of gene tree which relates the genetic sequences of viruses carried within one or more hosts. In this work, we consider viral phylogenies constructed from one sequence per infected individual, so that the tips of the are associated with both the viral sequence and the corresponding host.

1.1.4 Estimating transmission trees

Most applications of viral phylodynamics, including this project, aim to answer epidemiological questions (Pybus and Rambaut 2009; Volz, Koelle, and Bedford 2013). For example, phylodynamic methods have been used to investigate the degree of clustering (Hughes et al. 2009) and the effect of elevated transmission risk in acute infection (Volz, Koopman, et al. 2012) (a more thorough review is given below in subsection 1.1.6). For these applications, we are ultimately interested in the transmission tree, which is a representation of an epidemiological process (transmission), as opposed to the viral phylogeny, which represents a biological process (viral evolution). As discussed above in subsection 1.1.2, transmission trees and are in practice unknown, and must be estimated from available data. Here, we review some of the ways to perform such estimation.

In principle, transmission trees can be reconstructed by on-the-ground epidemiological methods, that is, by asking each person who they contacted. This is particularly relevant for sexually transmitted diseases such as HIV, where individuals are more likely to recall who they contacted and when (Klovdahl 1985). This kind of data is challenging to collect in detail. Most commonly, when applying phylodynamics in practice, the transmission tree is estimated from the viral phylogeny (Volz, Koelle, and Bedford 2013). As discussed above in subsection 1.1.3, the viral phylogeny is itself also estimated; however, for the moment we ignore this complication and describe methods for estimating the transmission tree if the viral phylogeny were known.

When we consider the fact that the viral phylogeny is not known with certainty, the methods just described follow a two-step procedure. The first step is to estimate the viral phylogeny, and the second step is to use it to estimate the transmission tree.

(Didelot, Gardy, and Colijn 2014) develop a Bayesian version of the two-step approach. They first estimate a time-scaled phylogeny from viral samples, then estimate the transmissions which took place along the phylogeny. Due to within-host evolution, the transmissions are allowed to occur anywhere along the branches, rather than being constrained to happen at branching points. However, the authors admit that their method requires sampling of every infected individual, although they indicate that it could be extended to relax this assumption.

A different approach is undertaken by Jombart *et al.* (Jombart et al. 2011), who build transmission trees directly from sequence data without the intermediate step of constructing a phylogeny. Their method finds the most likely geneology among the sampled sequences, assuming that the that the common ancestors to sampled isolates are themselves sampled. Although this may be a realistic assumption in the early stages of an epidemic of a slower evolving pathogen, it is unlikely for ancestors to be present among sequences sampled from an ongoing HIV epidemic . *Needs a reference*

Several alternative approaches have been developed which aim to incorporate available epidemiological data as well. Cottam *et al.* (Cottam et al. 2008) first built a viral phylogeny, then enumerated all transmission trees consistent with this phylogeny by labelling the internal nodes of the phylogeny in every possible way. Each of the putative transmission trees was assigned a likelihood based on infection time and geographic separation.

1.1.5 Tree shapes

The aim of viral phylodynamics is to glean some kind of knowledge, about the epidemic, the virus, or its hosts and their behaviour, by studying a phylogeny, most often a transmission tree. Phylogenies are complex objects, and it is not immediately obvious how to extract useful information from them with respect to fitting a parameter. Standard statistical methods, built for numeric data cannot be applied directly - for example, one cannot perform a regression of a parameter of interest against a phylogeny. Therefore, before we discuss exactly what phylodynamics can tell us about epidemics, and how it has been applied in the past, we will review some of the methods for quantifying the shapes of phylogenies and their similarity to each other.

Many tree summary statistics have been developed to assign numerical values to phylogenies based on their properties. One of the most widely used is Sackin's index **sha01990tree** which measures the imbalance or asymmetry in the tree.

1.1.6 Applications of phylodynamics

1.2 Contact networks

1.2.1 Overview

Epidemics spread through populations of hosts through *contacts* between those hosts. The definition of contact depends on the mode of transmission of the pathogen in question. For an airborne pathogen like influenza, a contact may be simple physical proximity, while for a sexually transmitted pathogen like HIV, contacts would be sexual partnerships. A *contact network* is a graphical representation of a host population and the contacts among its members. The *nodes* in the network represent hosts, and *edges* represent contacts between them.

Edges in a contact networks may be *directed*, representing one-way transmission risk, or *undirected*, representing symmetric transmission risk. For example, a network for an airborne epidemic would use undirected edges, because the same physical proximity is required for a host to infect or to become infected. However, a blood-borne infection spread through transfusions would use undirected edges, since the donor has no chance of transmitting to the recipient. Directed edges are also useful when the transmission risk is not equal between the hosts, such as with HIV transmission, where acting as the receptive partner carries a higher risk of infection than acting as the insertive partner. In this case, a contact could be represented by two directed edges, one in each direction between the two hosts, with the edges annotated by what kind of risk they imply. In fact, it is possible to represent an undirected edge by two symmetric directed edges. For this reason, we consider only contact networks with directed edges in the sequel. A directed contact network is shown in Figure 1.2.1 (left).

The path an epidemic takes through a contact network determines the topology of the transmission tree relating the infected hosts. The initially infected node who introduces the epidemic becomes the root of the tree. Each time a transmission occurs, the lineage corresponding to the donor host in the tree splits into two, representing the recipient lineage and the continuation of the donor lineage. This correspondence is illustrated in figure 1.2.1. It's important to note that, although the order and timing of transmissions determines the tree topology uniquely, the converse does not hold. That is, there are generally several orders of infection which could lead to the same topology, since the labels on the internal nodes of the tree are not available to the researcher.

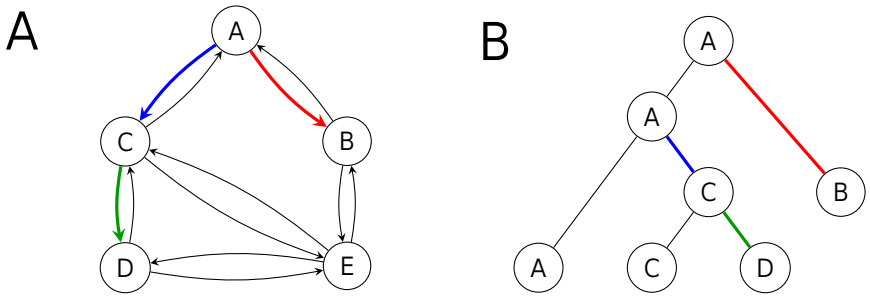

Figure 1.2: Illustration of epidemic spread over a contact network. On the left, a contact network with five hosts, labelled A through E. Directed edges indicate six symmetric contacts among the hosts. Coloured, bolded edges represent transmissions. The epidemic began with node A, who transmitted to nodes B and C. Node C further transmitted to node D, and node E was not infected. On the right, the transmission tree topology corresponding to this scenario. Note that individual B was sampled before the other infected individuals, resulting in a tree with heterochronous tips.

1.2.2 Models for contact networks

Throughout this section, the variable n will be used to refer to the number of nodes in the network.

An *Erdős-Rényi* (ER) network (Erdős and Rényi 1960), also known as a Bernoulli network, was the first network model described. It has a single parameter, p, which is the probability that any particular edge is present in the network. To construct an ER network, one simply chooses $p \times \binom{n}{2}$ distinct pairs of nodes and draws an edge between each pair. The average degree of a node in an ER network is equal to $p \times n$.

A *Barabási-Albert* (BA) network (Barabási and Albert 1999), incorproates the phenomenon of *preferential attachment* seen in real life networks. This means that new connections are more likely to involve nodes which already have a high number of connections - popular nodes tend to become more popular. In the formulation we consider here, BA networks have two parameters, m and α, which are used to construct the network via the following algorithm. The network begins as a single node, then the remaining $n - 1$ nodes are added one at a time. Each time a new node is added, it is connected to m other nodes. The probability of one of these connections involving an existing node of degree k is proportional to k^α. Note that in the original formulation (Barabási and Albert 1999), there was an additional parameter m_0 which indicated the number of initial vertices in the network, and the only value of α considered was 1. For our purposes, we fix $m_0 = 1$ but allow α to vary. We refer to α throughout this work as the *preferential attachment power* or just attachment power.

Networks produced by the BA model are *scale free*, which means that the probability of a node having k connections is proportional to k^γ for some constant γ. This is also called a *power law* degree distribution. An important remark on notation must be made

here: in network literature, the Greek letter α has often been used to refer to the power law exponent of the degree distribution, not the preferential attachment power. However, the paper defining the network model (Barabási and Albert 1999) uses γ for the power law exponent, and α for the attachment power, and we shall do likewise. This must be noted because there are reports in the literature of the power law exponent being as large as 4, which would seem to conflict with our choice (see subsection XX) to bound α above by 2. The reader should rest assured that it is the attachment power we are bounding, not the power law exponent.

WS and BA networks differ from ER networks in an important way: it is possible to explicitly calculate the likelihood of the ER model parameter p given an observed network, but this cannot be done for the other two models. This is because the probability of a particular edge occuring is always equal to p in an ER network, regardless of the presence or absence of any other edges. In other words, the edges can be viewed as a series of $\binom{n}{2}$ Bernoulli trials with success probability p, so that the likelihood of p given an observed graph with k edges is distributed as $\text{Binomial}\left(\binom{n}{2}, p\right)$.

1.3 Approximate Bayesian computation

1.3.1 Overview and motivation

Approximate Bayesian computation (ABC) is a statistical method designed to fit complex models, which cannot be fit using more conventional methods, to observed data (Marin et al. 2012; Sunnåker et al. 2013; Beaumont 2010) We shall make this precise below, but to fully describe and motivate ABC, it is necessary to first explain exactly what we mean by "fitting" a model. We will illustrate this concept with one of the simplest and most ubiquitous models: linear regression.

these are review articles, Beaumont is specific to popgen, the others are general

A linear regression is a model of the relationship between some data $\mathbf{x} = (x_1, \ldots, x_n)$ and outcomes $\mathbf{y} = (y_1, \ldots, y_n)$. This model assumes that the outcomes are linearly related to the data, modulo some noise introduced by, say, measurement errors and environmental fluctuations. It other words, there is a constant β such that $y_i = \beta x_i + \varepsilon_i$, where ε_i is the error associated with the outcome y_i. If we make the additional assumption that the errors are normally distributed, then the model takes the form

$$y_i = \beta x_i + \mathcal{N}(0, \sigma^2),$$

where $\mathcal{N}(0, \sigma^2)$ indicates a normally distributed random variable with mean 0 and variance σ. We will denote the probability density function (pdf) of this random variable by $f_{\mathcal{N}}(\cdot \mid \mu, \sigma)$. In this formulation, the coefficient β and the error variance σ are the two parameters

of the model. If the y_i are all independent, then for particular choics of β and σ, we can write down the probability density of observing $\mathbf{y}$ given $\mathbf{x}$.

$$f(\mathbf{y} \mid \mathbf{x}, \beta, \sigma) = \prod_{i=1}^{n} f_N(y_i - \beta x_i \mid 0, \sigma^2).$$

The higher the value of this probability density, the more likely the observations $\mathbf{y}$ are given $\mathbf{x}$ under the model. This gives us a natural criterion for choosing the parameters: we want to pick β and σ which define a model where the probability of our observed data is as high as possible. When performing such an optimization for fixed data, the density function just written is also called the *likelihood* of the parameters,

$$\mathcal{L}(\beta, \sigma \mid \mathbf{x}, \mathbf{y}) = f(\mathbf{y} \mid \mathbf{x}, \beta, \sigma).$$

The particular β and σ which optimize $\mathcal{L}(\beta, \sigma \mid \mathbf{x}, \mathbf{y})$ are called the maximum likelihood (ML) estimates.

ML inference makes use only of the data at hand, in this case $\mathbf{x}$ and $\mathbf{y}$, to estimate the parameters β and σ. However, it is frequently the case that the investigator has some additional *prior* information or belief about what β and σ are likely to be. For example, the instrument used to measure the $\mathbf{y}$ may have a known margin of error, or the sign of the slope may be obvious from previous experiments. Bayesian approaches to model fitting make use of this information by codifying the investigator's beliefs as a *prior distribution*, denoted $f(\beta, \sigma)$. The optimal parameters are then those which maximize the product

$$f(\mathbf{y} \mid \mathbf{x}, \beta, \sigma) f(\beta, \sigma) \propto f(\beta, \sigma \mid \mathbf{y}, \mathbf{x}).$$

Now that we have defined what it means to fit a linear regression, there remains the question of how to go about finding this optimal β value. Naïvely, we could simply try many different β and σ values, calculate the likelihood of each, and choose those which yield the highest value. This approach, though basic, falls under the umbrella of *numerical optimization* of the likelihood function. Of course, there is a whole field devoted to more sophisticated methods for exploring the parameter space, but they all boil down to the basic idea of trying out different values and choosing those which give the highest likelihood.

In the case of linear regression, there is another method we could use. We know from calculus that the maximum of $\mathcal{L}$ occurs either on the boundary of its domain, or at a point where its partial derivatives with respect to β and σ are both zero. Though we will not show it here, it turns out to be straightforward to find the β and σ values where the partial derivatives are zero. In fact, these values co-incide with the least-squares estimates of β and σ, which minimize the sum of the squared $x_i - \beta y_i$. However, the method of

directly minimizing the loss function with calculus is only applicable to a narrow class of simple models. For the majority, the likelihood function is too complicated to set the partial derivatives with respect to the parameters to zero and solve.

An approximate Bayesian computation approach to least-squares regression might be as follows. We will need to make an additional assumption: that the errors ε_i are normally distributed. That is, our linear model is now of the form

$$y_i = bx_i + \mathcal{N}(0, \sigma),$$

where $\mathcal{N}(0, \sigma)$ indicates a normal distribution with mean zero and variance σ. We do not know σ in advance, so this is another parameter we will need to estimate. There is nothing special about normal distributions - we could have chosen any other distribution we deemed appropriate.

The main idea of approximate Bayesian computation is that the "best" parameters will define a model which produces simulated data similar to the real data. Suppose we fix values of b and σ. Then, using the given data points x_i, we can generate simulated observations y_i^* by adding bx_i and a randomly chosen error drawn from $\mathcal{N}(0, \sigma)$.

1.3.2 Algorithms for ABC

Approximate Bayesian computation does not refer to a particular procedure for model fitting. Rather, ABC refers to the general strategy of choosing model parameters based on the resulting model's propensity to generate data resembling the real data. There are three main classes of ABC algorithm which have been developed so far: rejection, Markov chain Monte Carlo (MCMC), and sequential Monte Carlo (SMC).

All of these approaches require some common elements. First, as with all Bayesian methods, we are required to specify a *prior distribution*, denoted π, on the parameter space. The prior specifies what we already know or believe about the model parameters. Second, in order to compare simulated to observed data, we need to be able to summarize a data set in a numerical format. This is accomplished by a function, denoted η, which computes a vector of hopefully informative summary statistics on a data set. Third, we need a distance function ρ which tells us how similar two data sets are to each other, based on their summary statistics.

Continuing with the linear model example, we need to specify a prior $\pi(a, b, \sigma)$ on the three parameters. We do not have much certain information about these parameters except that σ has to be at least zero, but it seems reasonable to assume that extreme relationships are fairly rare, and that positive and negative correlations are equiprobable. Therefore, we will let a, b, and σ be independent, a and b be normally distributed, and σ be log-normally

distributed. That is,

$$\pi(a, b, \sigma) = \begin{cases} \Pr[\mathcal{N}(0,1) = a] \cdot \Pr[\mathcal{N}(0,1) = b] \cdot \Pr[\mathcal{N}(0,1) = \log \sigma] & \sigma > 0 \\ 0 & \sigma \leq 0. \end{cases}$$

For the vector of summary statistics, we will use the mean and variance of the simulated data,

$$\eta(\mathbf{y}) = \langle \mathrm{E}[\mathbf{y}], \mathrm{Var}[\mathbf{y}] \rangle .$$

Finally, for the distance function ρ we take the standard Euclidian distance.

Rejection ABC is the simplest method, and also the one which was first proposed (Rubin et al. 1984). Effectively, it comes down to the approach described in the previous subsection of guessing parameter values until one is close enough to the truth. More specificially, a possible set of parameters θ is drawn from the prior distribution, and a simulated data set z is generated from the model with those parameters. If the distance between the simulated data set and the real data, $\rho(\eta(y), \eta(z))$, is small enough, then we accept θ as a sample from the posterior. This can be repeated until as many samples as desired are obtained.

The second method is ABC-MCMC. This is similar to ordinary Bayesian MCMC, except that a ratio of distances to the observed data replaces the likelihood ratio. The algorithm begins by sampling a single vector of parameter values θ from the prior distribution $\pi(\theta)$. It then proceeds iteratively: a new parameter vector θ^* is chosen according to a proposal distribution $q(\theta^* \mid \theta)$. The proposal distribution q is often taken to be a Gaussian centred at θ. Then θ^* is accepted as the new θ with probability

$$\max(1, \mathrm{TODO}),$$

or discarded otherwise. This process is iterated until some stopping criterion is reached, typically a simple limit on the number of steps. After some initial number of iterations, known as *burn-in*, parameters θ are routinely sampled. Since points in parameter space are visited in proportion to their posterior probability, these samples can be taken to approximate the posterior distribution on θ, and can be used to calculate point estimates and confidence intervals.

The most recently developed class of algorithms for ABC is sequential Monte-Carlo (SMC) (Sisson, Fan, and Tanaka 2007). As with the other two classes, we want to eventually obtain a sample from the posterior distribution $f(\theta \mid D)$. The idea of SMC is to begin with a sample from a distribution we know, most often the prior, and approach the posterior smoothly by progressing through a series of intermediate distributions.

Chapter 2

Body of Thesis

2.1 Objective

Our objective is to develop a method to estimate structural parameters of the contact network underlying an observed transmission tree.

2.1.1 Prior work

The present study is closely related to three groups of work with distinct objectives, which will be reviewed in detail below.

The first and largest group of related studies are phylodynamic investigations of epidemiological parameters such as transmission rate, recovery rate, and basic reproductive number (Pybus and Rambaut 2009; Volz, Koelle, and Bedford 2013). Like our work, these studies make inferences about epidemiological processes from the genetic diversity of virus populations, which is usually represented in the form of a phylogeny. The majority of these employ a Bayesian MCMC approach to infer parameters of an epidemiological model whose likelihood can be calculated, most often some variation of the birth-death (Kendall 1948) or coalescent (Kingman 1982) models. Stadler *et al.* (Stadler et al. 2011) develop a formula for the likelihood of a phylogeny with heterochronous tips under the birth-death model, which has been used to estimate the basic reproductive number of several viral epidemics (Stadler et al. 2011). However, the birth-death model is cannot tell us anything about population structure, as it assumes that every individual becomes infected at the same rate. Volz (**volz2012complex**) writes down the likelihood of a heterochronous phylogeny under a coalescent model with arbitrarily complex population dynamics. This opens the door to more complex inferences about population structure, as the population can be partitioned into compartments with different transmission and recovery rates, but still assumes that each compartment is homogeneously mixed. In other words, the coalescent model can tell us about the *global* structure of a population, such as whether there exists a high-risk

subgroup, but not about the *local* structure, such as the average number of contacts each individual has.

A second, more recent group of studies has evaluated the effect of network structure on transmission tree shape. The use of models which assume a *panmictic* (that is, homogeneously mixed) population in phylodynamics has become widespread, so it is natural that some researchers have investigated the effects of this assumption. In particular, since phylodynamic methods use phylogenies as their data source, several studies have examined the shapes of phylogenies arising from non-panmictic populations. O'Dea and Wilke (2010) simulated epidemics over networks with four types of degree distribution. They then estimated the Bayesian skyride (Minin, Bloomquist, and Suchard 2008) population size trajectory in two ways: from the phylogeny, using MCMC; and from the incidence and prevalence trajectories, using the method developed by Volz *et al.* (**volz2009phylodynamics**). They found that the concordance between the two skyrides, as well as the relationship between the skyride and prevalence curve, was qualitatively different for each degree distribution. Leventhal et al. simulated transmission trees over Erdős-Rényi (ER), Watts-Strogatz (WS), Barabási-Albert (BA), and full networks with fixed number of nodes and mean degree. They calculated Sackin's index of the simulated trees while varying the epidemic, network, and sampling parameters, and found that the relationship between these parameters and Sackin's index varies considerably among the different network models. In summary, studies in this group have demonstrated that network structure profoundly influences tree shape, but have not attempted to quantitatively infer network parameters from observed trees.

Finally, a third group of studies has used Bayesian methods to infer a structural network parameter from observed infection and recovery times. This third group is most similar in aims to our own work; rather than using epidemiological observations, we employ viral phylogenies. The pioneering study in this group was by Britton and O'Neill (2002), who developed a Bayesian method to infer the p parameter of an ER network, along with the β and γ parameters of susceptible-infected (SI) model. Their method is able to use either infection and removal times, or removal times only. However, it is designed for only a small number of observations (15 and 42 cases in their applications), and their estimates of p for real outbreaks were mostly uninformative (95% confidence intervals [0.11-0.96] and 0.055-0.96]; p is bounded in [0, 1]). Groendyke, Welch, and Hunter (2011) significantly updated and extended the methodology of Britton and O'Neill, and applied it to a measles outbreak affecting 188 individuals. They were able to obtain a much more informative estimate of p, although this data set included both symptom onset and recovery times for all individuals. They also assumed that the entire network was infected, so that the network size was exactly 188. It is unclear how well their method would scale to networks with thousands of nodes.

2.2 Methods

2.2.1 Programs

Most of the computer programs used for this work were written in the C programming language. Contact networks were generated using the *igraph* library (Csardi and Nepusz 2006), which was also used to store phylogenetic trees. Hash tables, and the dynamic programming matrices for computing the tree kernel, were stored using Judy arrays (Baskins 2004). The GNU Scientific Library (GSL) (Gough 2009) was used to generate random draws from probability distributions, and to perform the bisection step in the ABC-SMC algorithm.

Epidemic simulation over a network

I implemented method of (**gillespie1977exact**) for simulating epidemics, and the corresponding transmission trees, over static contact networks. This method has been applied previously for the same purpose (Robinson et al. 2013; Leventhal et al. 2012), however no existing open source implementations were available.

Let $G = (V, E)$ be a directed contact network. Each directed edge $e = (u, v)$ in the network is associated with a transmission rate β_e, which indicates that, once u becomes infected, u will infect v with rate β_e. In other words, the time between u becoming infected and the infection passing from u to v is a random variable with distribution Exponential(β_e). Note that v may become infected before this time has elapsed, if v has other incoming edges. Each vertex v also has a removal rate γ_v, which is the rate at which v is removed from the population after becoming infected. Removal may correspond to death or recovery with immunity, or a combination of both, but in our implementation recovered nodes never re-enter the susceptible population. Borrowing a term from HIV epidemiology, a *discordant edge* in G is an edge (u, v) where u is infected and v is uninfected.

To describe the algorithm, we introduce some notation and variables. Let $\text{in}(v)$ be the set of incoming edges to v, and $\text{out}(v)$ be the set of outgoing edges from v. Let I be the set of infected nodes in the network, R be the set of removed nodes, and S be the remaining susceptible nodes. Let D be the set of discordant edges in the network, β be the total transmission rate over all discordant edges, and γ be the total removal rate of all infected nodes. That is,

$$\beta = \sum_{e \in D} \beta_e, \quad \gamma = \sum_{v \in I} \gamma_v.$$

The variables S, I, R, D, β, and γ are all updated as the simulation progresses, but since these updates are very straightforward we do not write them explicitly in the algorithm.

When a new node v is infected, it is deleted from S and added to I, any formerly discordant edges in $\in(v)$ are deleted from D, and edges in $\text{out}(v)$ to nodes in S are added to D. If v is later removed, it is deleted from I and added to R, and any discordant edges in $\text{out}(v)$ are deleted from D. In both cases, the variables β and γ are updated to reflect the changes.

The full algorithm is shown in Algorithm 2.2.1. The transmission tree T is simulated along with the epidemic. We keep a map called tip, which maps infected nodes in I to the tips of T. The variable n counts the number of nodes, both extant and internal, in T. The simulation continues until either there are no discordant edges left in the network, or we reach a user-defined cutoff of time ($t_{\max}$) or number of infections ($I_{\max}$).

Algorithm 1 Simulation of an epidemic and transmission tree over a contact network

```
infect one node v at random
let T be a single node with index 1
tip[v] ← 1
n ← 1
t ← 0
while D ≠ ∅ and |I| + |R| < I_max and t < t_max do
    s ← min(t_max − t, Exponential(β + γ))
    for v ∈ tip do
        extend the branch length of tip[v] by s
    end for
    t ← t + s
    if t < t_max then
        if Uniform(0, 1) < β/(β+γ) then
            choose an edge e = (u, v) from D with probability β_e/β and infect v
            add nodes with labels n + 1 and n + 2 to T
            connect n + 1 and n + 2 to tip[v] in T, with branch lengths 0
            tip[v] ← n + 1
            tip[u] ← n + 2
            n ← n + 2
        else
            choose a node v from I with probability γ_v/γ and remove v
            remove v from tip
        end if
        update S, I, R, D, β, and γ
    end if
end while
```

Phylogenetic kernel and normalized lineages-through-time

The tree kernel developed in (Poon et al. 2013) provides a comprehensive similarity score between two phylogenetic trees. The kernel computes the dot-product of two feature vectors, corresponding to the two trees, in the infinite-dimensional feature space of all possible

subset trees with branch lengths. I implemented the fast algorithm developed in (Moschitti 2006), which first enumerates all pairs of subtrees with the same number of leaf children, and then computes the kernel by dynamic programming.

In addition, we implemented a modified version of the normalized lineages-through-time statistic developed in (Janzen, Höhna, and Etienne 2015), which uses piecewise linear functions instead of step functions for the lineages-through-time plots. This modification is to address a potential inconsistency for trees of different sizes, illustrated in Figure 2.1.

Figure 2.1: Comparison of original formulation of normalized lineages-through-time, developed in (Janzen, Höhna, and Etienne 2015), with our modified version using linear interpolation. Here, the red and blue trees both have uniformly spaced branching times. Using step functions (left), the nLTT of the two trees is non-zero due to the differing numbers of internal branches. Using linear interpolation, the nLTT is zero (right). The lines on the right graph have been offset for visibility.

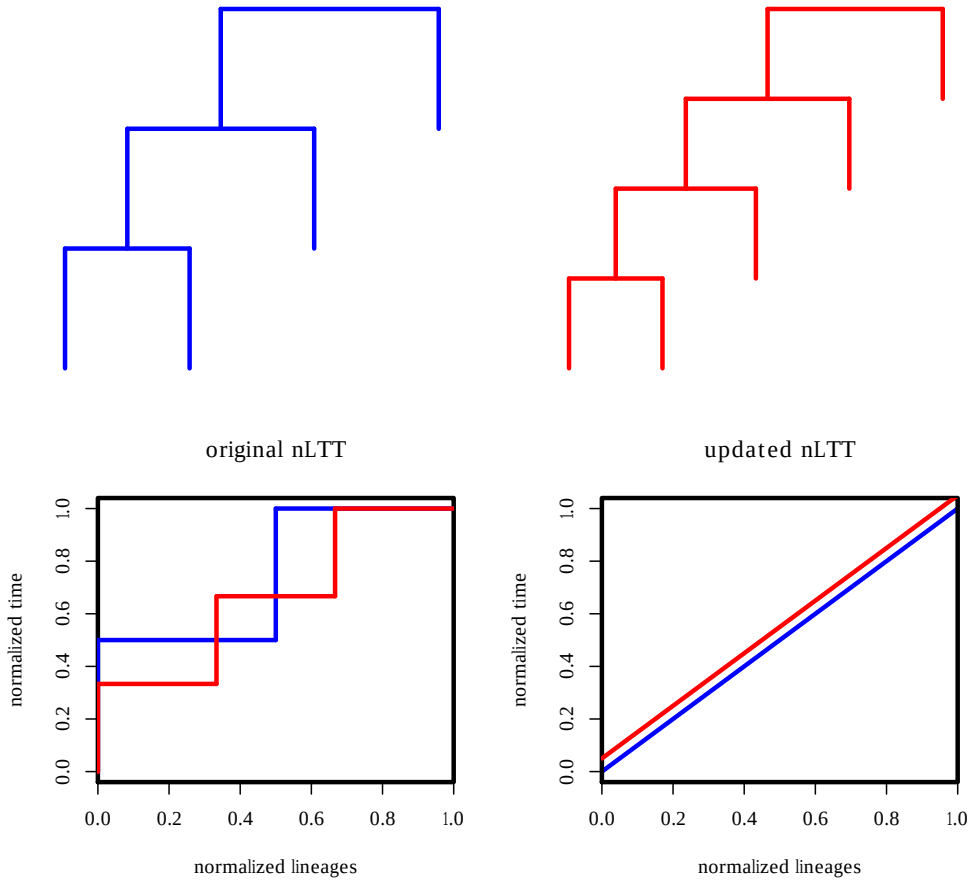

Adaptive sequential Monte-Carlo approximate Bayseian computation

I implemented the adaptive sequential Monte-Carlo (SMC) algorithm developed by Del Moral *et al.* (Del Moral, Doucet, and Jasra 2012) for approximate Bayesian computation.

For ease of exposition, we simplifiy the notation of Del Moral *et al.*by dropping the subscripts on the variables which indicate the current iteration of the algorithm. Instead, we will add a superscript * to indicate the value of the variable which will be used in the next iteration (this should become clear later on). Let $\{\theta_i\}_{i=1}^N$ be a set of N particles, which are particular choices of the model parameters θ. For each particle θ_i, let $\left\{X_{i,j}\right\}_{j=1}^M$ be a set of M simulated datasets, generated from the model with parameters θ_i. Let $\{W_i\}_{i=1}^N$ be weights associated to each particle. Let d be a distance measure on data sets, so that $d(x,y)$ is smaller the more similar x and y are to each other. Let ε be the tolerance level which indicates whether a data set is "close" to the observed data. That is, if $d(x,y) < \varepsilon$, we will say that x and y are close, otherwise they are distant.

Next, we calculate the next tolerance ε^*. Before we explain how this is done, we first need to define how we adjust the weights on the particles. As explained above (see subsection 1.3.2), the idea of sequential Monte-Carlo is to begin with the prior distribution π, progress smoothly through a series of intermediate distributions $\pi_1, \ldots, \pi_{n-1}$, and eventually arrive at the target posterior distribution π_n. In the kth iteration, the distribution π_k is approximated by the particles and their weights.

In contrast to most existing sequential Monte-Carlo methods, this algorithm does not require the user to specify a sequence of decreasing tolerances to approach the target posterior distribution. Rather, the tolerances are computed adaptively at each step, starting from infinity at the first iteration.

The algorithm may be stopped when the tolerance reaches a user-defined final value, or when the rate of acceptance of the Metropolis-Hastings kernel reaches a user-defined threshold. Following a heuristic applied by the authors (Del Moral, Doucet, and Jasra 2012), we used the latter stopping criterion, accepting the SMC approximation to the posterior when the MCMC acceptance rate dropped below 1.5%.

2.2.2 Simulation experiments

Identification of separable parameters in kernel space

Recall that our approximate Bayesian computation approach to fitting contact network models involves simulating transmission trees under a wide variety of parameter values, and then comparing these simulated trees to the true transmission tree. Values which produce trees similar to the observed transmission tree are distinguished as more likely than values which produce trees very different from the truth. In order for this type of analy-

sis to succeed, it is critical that different parameter values produce different looking trees. Otherwise, if many different values produce trees which are too similar to each other, it will be impossible to distinguish which value is most consistent with the real tree. Just as importantly, trees simulated with similar parameter values must be similar to each other. In mathematical terms, we require the trees simulated from distinct parameter values to be *separable* in tree space. The concept of separability is illustrated in Figure 2.2.

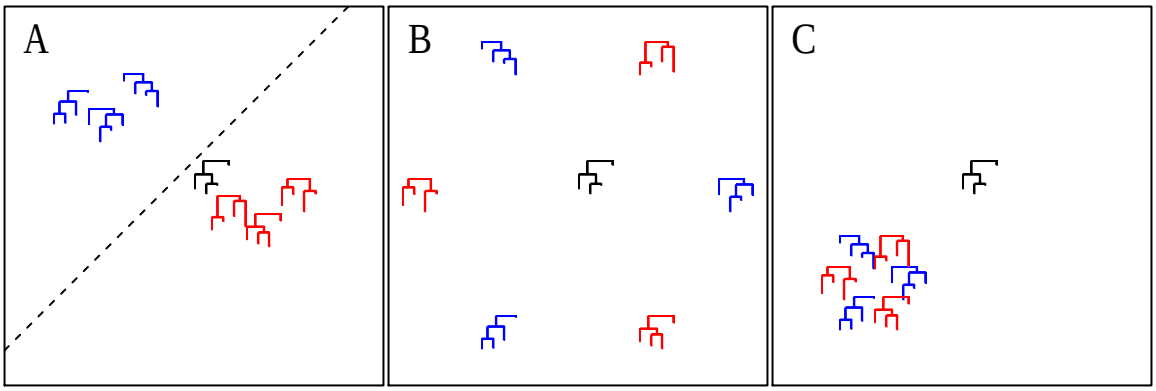

Figure 2.2: Separable versus non-separable parameters in kernel space. Trees have been simulated under three sets of parameters, represented as blue, red, and green. An observed tree is shown in black. Trees are layed out such that the distance between two trees corresponds to their similarity. In panel A, trees from the same parameter set are similar to each other, but different from other trees. The true tree is most consistent with the red parameters. In panels B and C, trees from the same parameter set are not similar to each other (B), or trees from different parameter sets are similar to each other (C). It's difficult to say which parameters the true tree is most consistent with.

Before undertaking a complete ABC analysis, I analysed four simple contact network models to determine whether their parameters could be separated in tree kernel space. The four models are described in detail in subsection 1.2.2 of the introduction. Briefly, they are: random networks, where each possible contact has a fixed probability of occuring; preferential attachment networks, where highly connected nodes tend to attract more contacts; small world networks, where nodes are connected to their immediate neighbours and the occasional far-flung contact; and full networks, where every possible connection is present. I will describe here only the procedure and results for the preferential attachment networks. The details of the other three types of graph can be found in the supplemental materials. A graphical schematic of the analysis undertaken here is given in Figure 2.2.2.

The method of testing for separability was described previously in (Poon 2015), but I will reiterate it here for completeness. As a concrete example, consider the attachment power parameter α of the preferential attachment networks. This parameter describes the strength of attraction to highly connected nodes and is bounded below by zero indicating no extra attraction. By qualitative observation, I determined that a power of 2.0, which

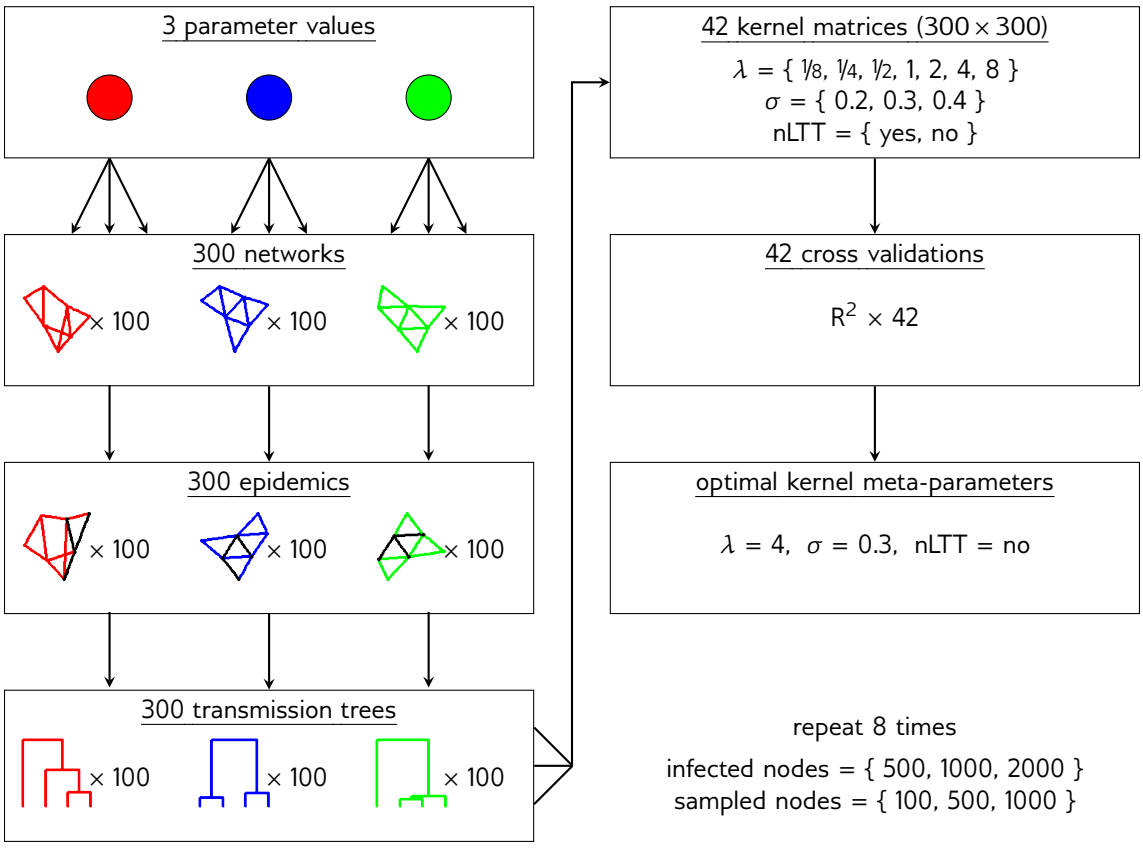

Figure 2.3: Schematic of first set of simulation experiments to determine separable parameters in kernel space, along with optimal tree kernel meta-parameters.

produced networks with very few "hub" nodes with extremely high degree, was a suitable upper bound (see Figure 2.2.2). Therefore, I chose to test the values 0.5, 1.0, and 1.5 for separability. The other parameters were fixed: the number of nodes in the network was 5000, and the mean degree of each node in the network was four. As discussed in subsection 1.2.2, this is the smallest mean degree value for preferential attachment networks which produces networks which are more than trees.

For each of the values of α, I generated 100 networks on 5000 nodes. An epidemic was simulated over each network (see subsection X) until 1000 nodes were infected, and 500 of those infected nodes were sampled to form a transmission tree. This resulted in 300 total simulated transmission trees - 100 for each of the three values of α. The data generation steps are shown on the left side of Figure 2.2.2. Next, I computed the tree kernel (Poon et al. 2013) (see subsection 1.1.5) for each pair of trees. These values were placed into a 300 × 300 kernel matrix, where the value at the (i, j)th position was the tree kernel of the ith and jth trees.

The tree kernel provides a pairwise similarity score between two trees. The higher the kernel score, the more similar the trees are to each other. Therefore, to have separability, we need trees simulated with the same value of α to have high kernel scores with each other,

but low kernel scores with trees from different α values. We can visually check whether or not this is true by laying out the trees as points on a graph, in such a way that trees with high scores are close to each other, but trees with low scores are far apart. This is accomplished by performing a kernel principal components analysis (kPCA) (Schölkopf, Alexander Smola, and Müller 1998) on the kernel matrix. Briefly, ordinary principal components analysis (PCA) finds a lower dimensional representation of points in a high dimensional space which preserves as much of the variation in the data as possible. kPCA performs the same task, but using the dot products of each pair of points as input, instead of the data points themselves. A two-dimensional kPCA projection of the simulated trees is shown in Figure 2.3.1. The scenario just described - 500 samples from 1000 infected nodes - is the central panel. To ensure that the method could be used in a variety of contexts, the same analysis was performed with 500 and 2000 infected nodes, as well as 100 and 1000 sampled tips.

The next step was to quantify how well trees simulated with different α values could be distinguished from each other. As described previously (Poon 2015), this was done by assessing the accuracy of a support vector machine regression (SVR) (Alex Smola and Vapnik 1997). Briefly, an SVR operates by finding a hyperplane (in two dimensions, a line) such that the deviation of most of the data points from the line is less than some prescribed threshold. Points further away than this threshold are ignored in the model. I performed 1000 replicate 2-fold cross-validations of an SVR predicting preferential attachment power on the simulated trees, using the *ksvm* function from *kernlab* (Karatzoglou et al. 2004). That is, the SVR was trained on a random subset of 150 trees, and then used to predict α of the remaining 150 trees. The predictions were correlated against the true values of α to obtain an R^2, and this procedure was repeated 1000 times with different subsets of trees.

The cross-validation had the dual purpose of providing a means to selecting the optimal meta-parameters to the tree kernel (see subsection 1.1.5) - they are be those which provide the highest average R^2. To this end, the cross-validation was repeated for several values of λ and σ as shown in Figure 2.2.2 Each combination was evaluated with and without multiplying the tree kernel by the normalized lineages-through-time (nLTT) statistic, and was further repeated for the scenarios with differing numbers of infected and sampled nodes described above. To ensure that the tree kernel was the most appropriate similarity measure to use for ABC, we also computed the R^2 of α against Sackin's index, a widely used tree balance statistic (see subsection 1.1.5), by the same cross-validation procedure.

Grid search

The previous set of simulations were intended to investigate which contact network parameters could and could not be inferred by examining transmission trees. However, they

tell us nothing about the accuracy or precision we might expect when inferring those parameters numerically. As illustrated in Figure 2.5, the ideal situation is one where we are accurate and precise, and the worst situation is when we are precise but not accurate.

Figure 2.6 shows a schematic of this experiment. A number of representative values, here denoted k, were chosen for the parameter of interest. In the case of preferential attachment power α, I chose $k = 8$ testing values, namely $0, 0.25, \ldots, 2.0$. For each of these values, ten networks on 5000 nodes were generated, an epidemic of 1000 nodes was simulated over each, and a transmission tree of 500 tips was sampled. The resulting $10 \times k$ simulated transmission trees were referred to as the *testing trees*. In addition, I chose a further $n \gg k$ training values spanning the range of the parameter. For α, these were $0, 0.01, \ldots, 2.0$. Fifteen trees were simulated in the same manner for each of these values, referred to here as *training trees*.

For each of the testing trees, I computed the tree kernel with all of the training trees. This resulted in 15 kernel scores per training value. The training value with the highest median kernel score was used as a point estimate of the testing value. The kernel scores were then normalized to lie in [0, 1], and an interval was found which contained 95% of the area under the curve and was of minimal width. This was used as a 95% confidence interval for the parameter.

Approximate Bayesian computation

Our final set of simulation experiments was to test the ABC-SMC algorithm on simulated data. For each replicate, we generated a network on 5000 nodes, simulated an epidemic over that network until 1000 nodes were infected, and sampled either 500 or all 1000 of those nodes to form a transmission tree. Priors were specified as follows: for the total number of nodes in the network, Uniform$(1000, 10000)$; for the number of infected nodes, Uniform$(500, 2000)$; for the preferential attachment power, Uniform$(0, 2)$. The mean degree of nodes in the network was fixed at either 4, 10, or 16. The algorithm was run with 1000 particles, and was stopped when the MCMC acceptance probability dropped below 1.5%.

2.2.3 Applications

HIV in British Columubia

2.3 Results

2.3.1 Separable parameters

Our first simulation-based experiment was designed to determine which network model parameters were potentially estimable by kernel-ABC. To do this, we simulated trees under three distinct values of each parameter of interest, and evaluated the accuracy of a kernel-SVM classifier for the parameter. This is the same approach taken by Poon (2015), and has the dual purpose of allowing us to identify the optimal kernel meta-parameters σ and λ. The parameters of the ER, WS, and BA network models were examined, but we will discuss only the results for the α and prevalence parameters of the BA model in the main text. The results for the remaining models and their parameters can be found in the supplemental material.

In Figure 2.3.1, we show that trees simulated under different values of α are visibly quite distinctive. In particular, higher values of α result in networks with a small number of highly connected nodes (see Figure 2.2.2) which, once infected, are likely to transmit to many other nodes. This results in a more unbalanced, ladder-like structure in the phylogeny. Kernel-principal components analysis (PCA) projections show that all three α values are well separated from each other under several different sampling scenarios (Figure 2.3.1). With smaller trees, it becomes harder to visually disinguish $\alpha = 0.5$ from $\alpha = 1.0$ using the first two principal components.

With suitably chosen meta-parameters, the accuracy of the kernel-SVM classifier for α was very high under a variety of prevalence and sampling scenarios (Figure 2.3.1). Accuracy was highest, with R^2 values above 0.95, for the largest trees and complete sampling (bottom center panel). However, even for trees of size 100 sampled from an epidemic on 2000 nodes, the R^2 was above 0.8 (top right panel). In all cases, the accuracy of a Sackin's index-based classifier was also quite high, at about 0.75. The fact that Sackin's index is informative of α was unsurprising, given the clear differences in tree balance observed under different α values. The normalized lineages-through-time (nLTT) statistic (Janzen, Höhna, and Etienne 2015) did not improve the classifier, but rather slightly reduced the R^2 in most cases.

We also considered the possibility of inferring the number of infected nodes, or *prevalence*, under this model. All parameters except I were fixed at the following values: $N = 5000$, $\alpha = 1.0$, and $m = 2$. As shown in Figure 2.3.1, the prevalence had no obvious effect on the tree shape. However, a kernel-SVM classifier was able to distinguish the number of

infected nodes with high accuracy ($R^2 > 0.9$; Figure 2.3.1). Moreover, the use of the nLTT statistic improved classification accuracy by a small amount, in contrast to the results for α. In contrast, a Sackin's index-based classifier displayed extremely poor performance ($R^2 < 0.1$, not shown).

It is important to note that, if we cut off the epidemic simulation when 500 nodes are infected, the resulting tree will be shorter (in calendar time) than if we continue until 2000 nodes are infected. However, this information is not used when building the classifier, since the branch lengths in each tree are scaled by their mean. Therefore, the high performance of the classifier is due to structural differences captured by the tree kernel, rather than the trees simply having different heights.

2.3.2 Accuracy of marginal estimates

We used grid search to obtain *marginal* estimates for each network parameter while holding all other parameters fixed. We observed that kernel scores were highest at the values of α on the grid closest to the true values, as shown in Figure 2.12. However, there was a much stronger spike in kernel scores near the true value for $\alpha = 1.0$ and 1.25. This is recapitulated when we look at the accuracy of point estimates obtained by taking the grid value with the highest median kernel score. As shown in Figure 2.13, while the estimates are generally close to the true value, they are much closer for $\alpha = 1.25$ than for the other values.

2.3.3 Accuracy of estimates with full ABC

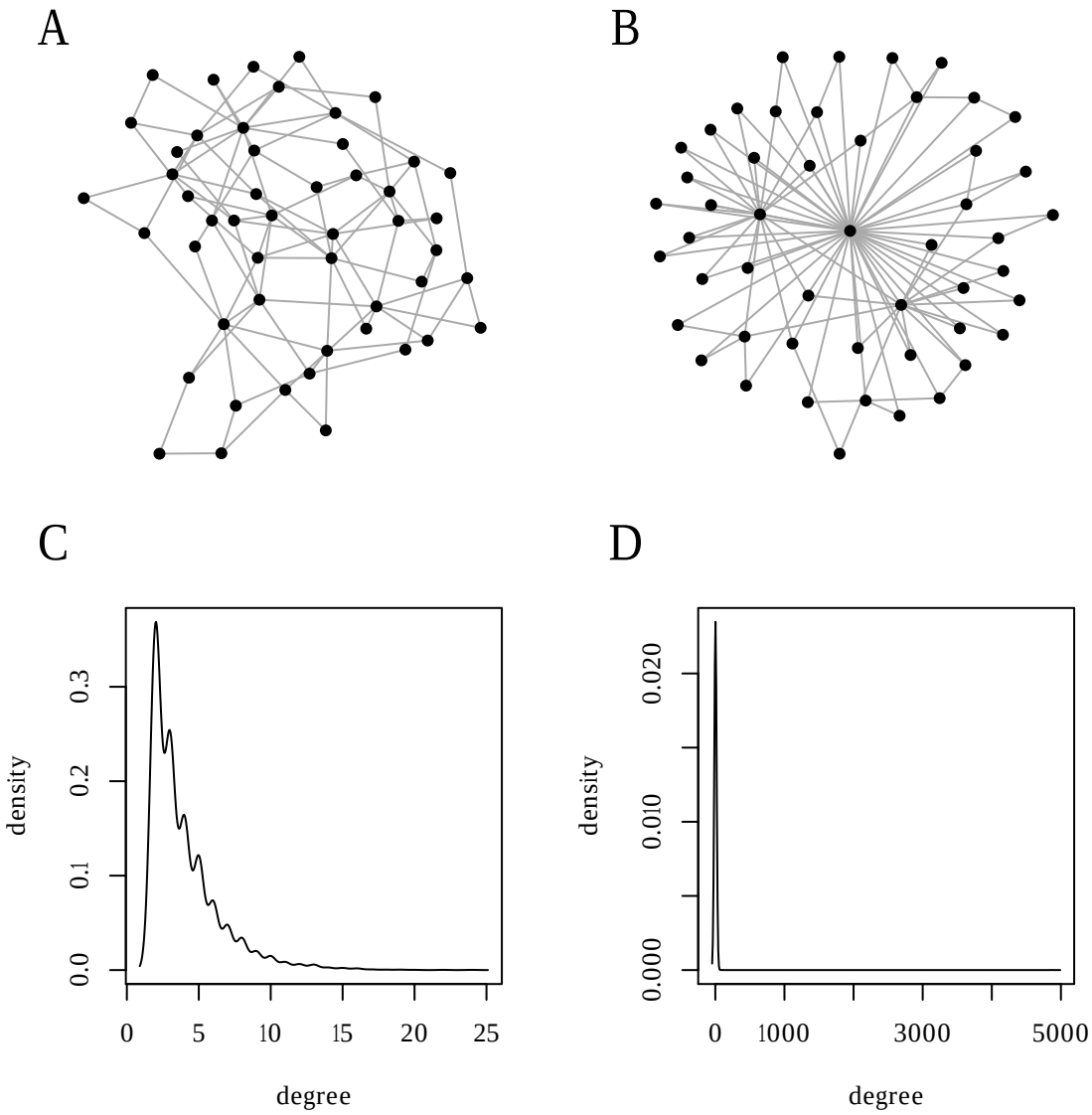

Figure 2.4: Qualitative justification for choice of zero and two as lower and upper bounds on preferential attachment power α. (A) Preferential attachment network on 50 nodes with $\alpha = 0$, the lower bound enforced by the model. (B) Preferential attachment network on 50 nodes with $\alpha = 2$, where a few nodes have very high degree but the majority have very low degree. (C) Density plot of node degrees in a 5000-node network with $\alpha = 0$. The maximum degree of a node in this network was 24. (D) Density plot of node degrees in a 5000-node network with $\alpha = 2$. The maximum degree of a node in this network was 4942.

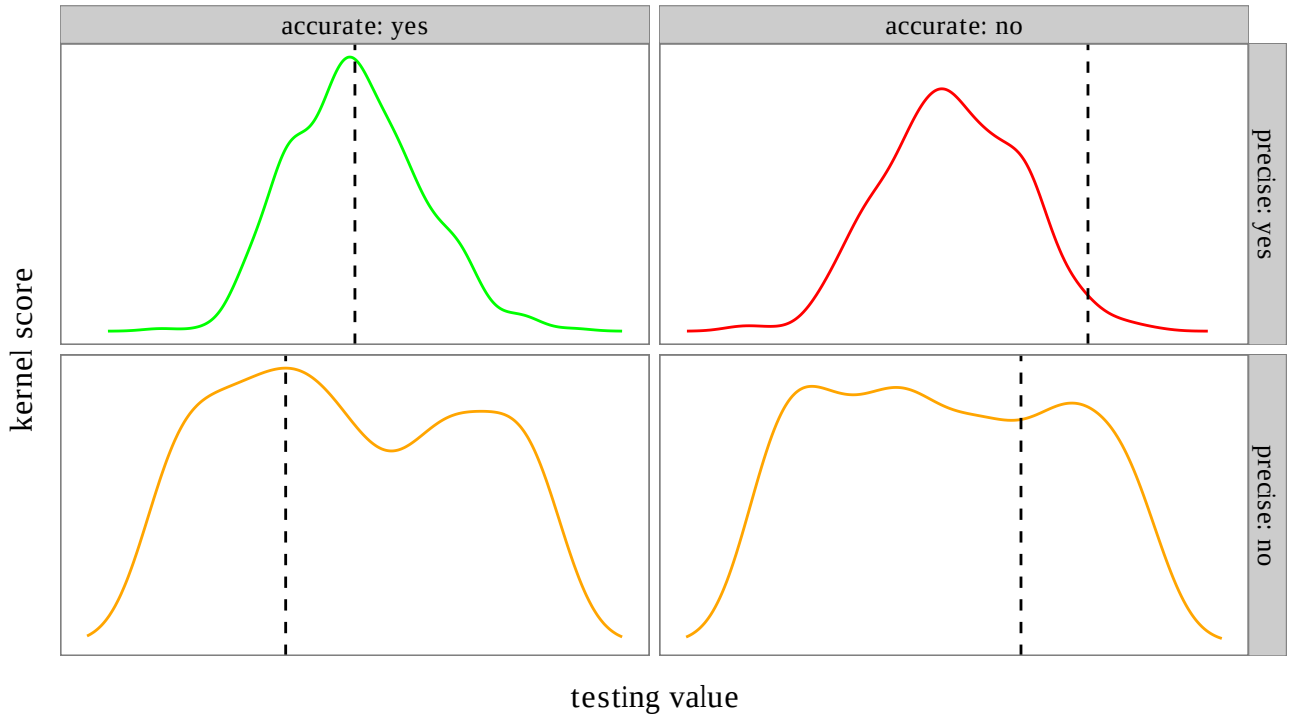

Figure 2.5: Illustration of accurate vs. precise kernel score estimates

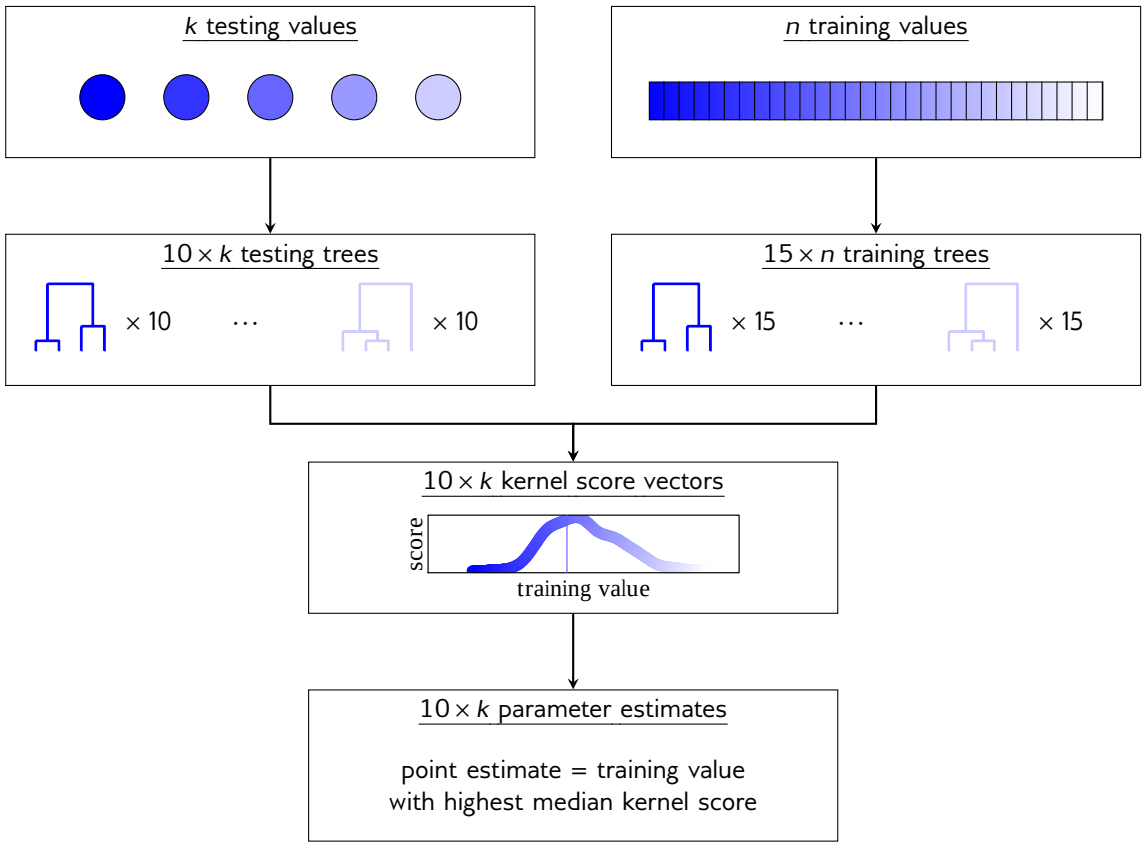

Figure 2.6: Schematic of grid search simulation experiments.

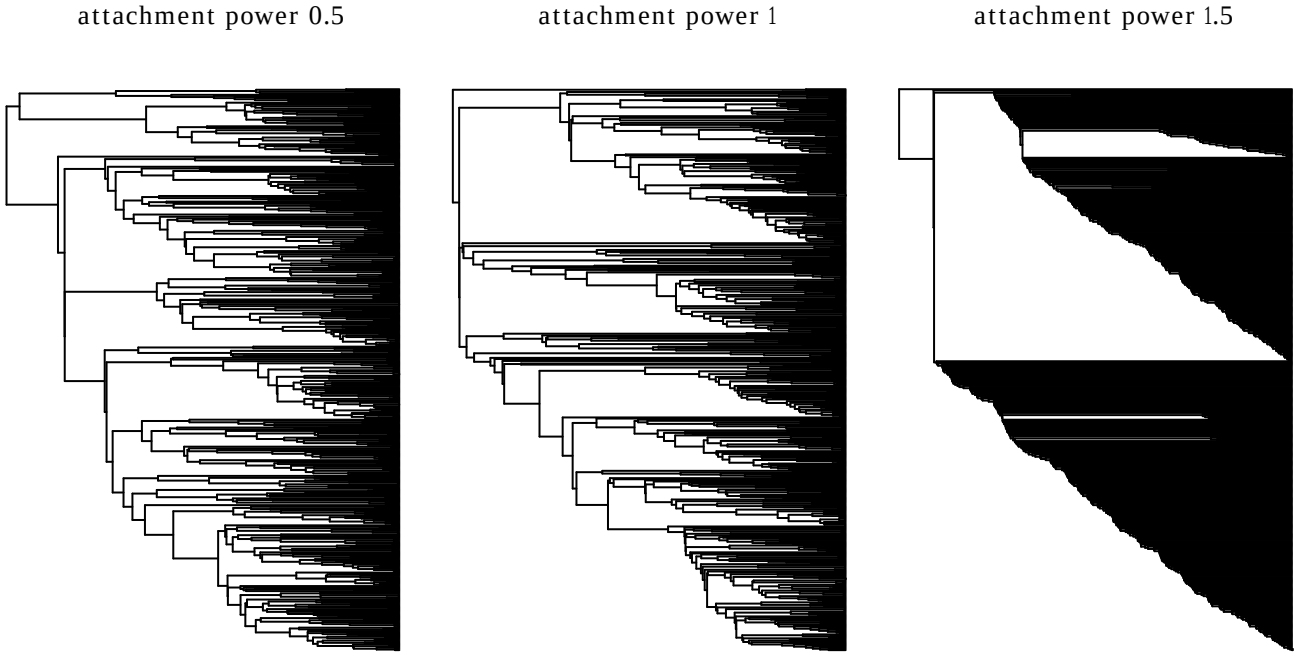

Figure 2.7: Epidemics of 1000 infected were simulated on BA networks of 5000 nodes, with α equal to 0.5, 1.0, or 1.5. Transmission trees were created by sampling 500 infected nodes. Higher α values produce networks with a small number of highly-connected nodes, which results in a highly unbalanced, ladder-like tree structure.

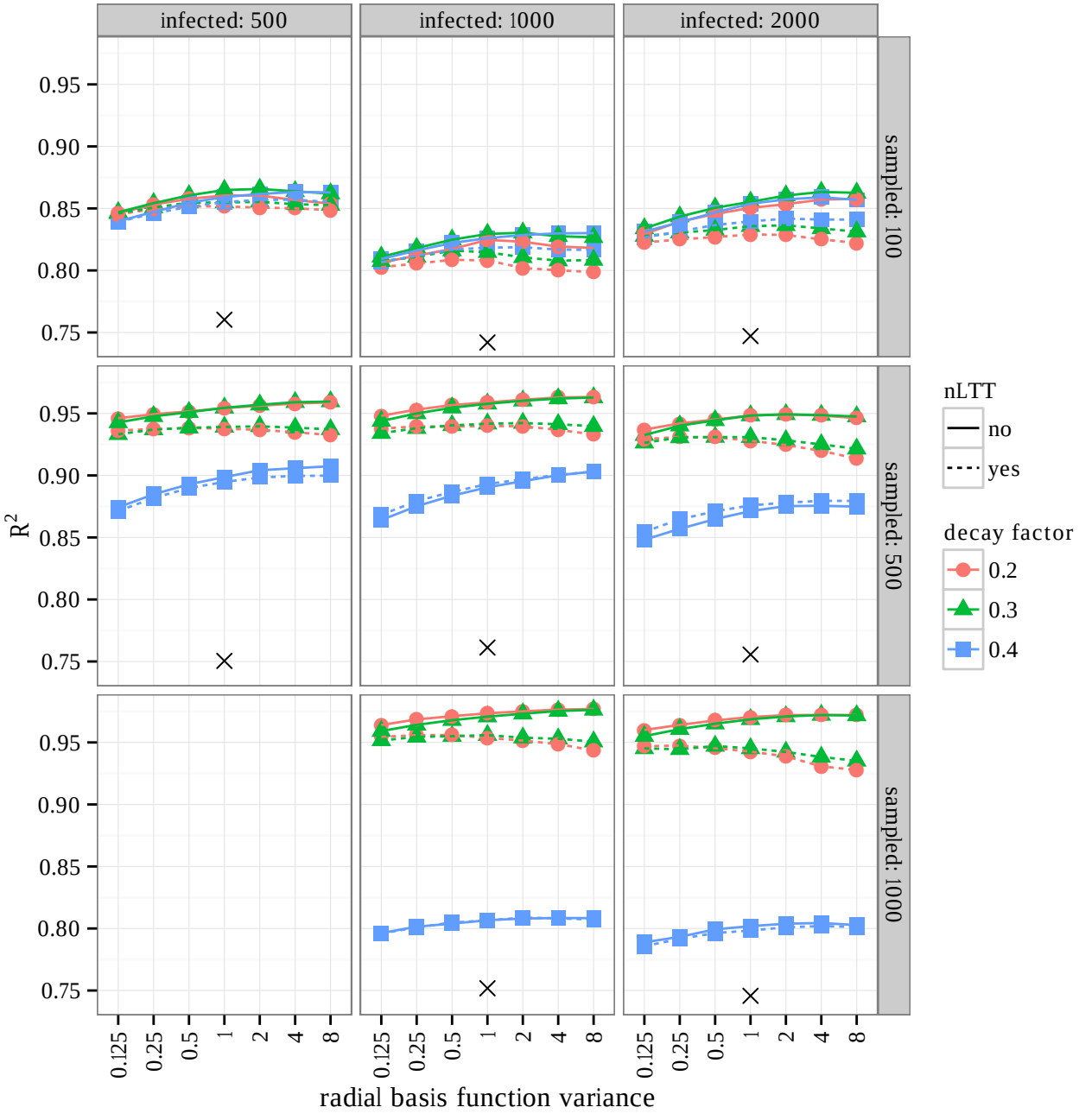

Figure 2.8: Cross-validation performance of kernel support vector machine classifier for preferential attachment power.

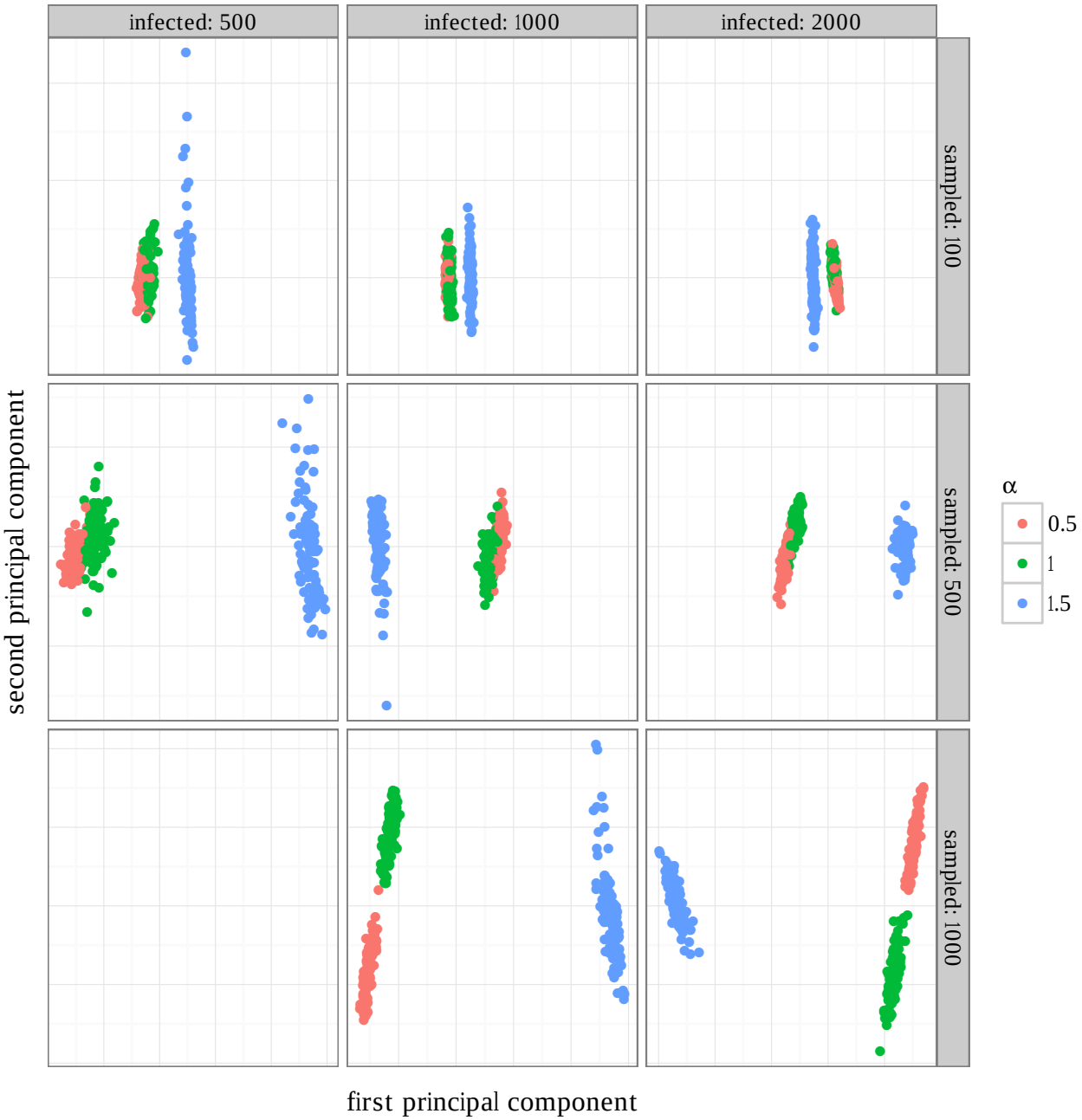

Figure 2.9: Projection of the kernel matrix for different preferential attachment power values onto its first two principal components, for eight simulation scenarios. Each point corresponds to a simulated transmission tree, and is coloured by preferential attachment power. Facets are number of infected nodes (horizontal), and number of sampled tips (vertical). The parameters to the tree kernel were $\lambda = 0.3$ and $\sigma = 4$, and the nLTT was not used. Qualitatively, trees with a larger number of tips are easier to separate in kernel space, regardless of what sampling proportion they represent. In all cases, the highest attachment power can be separated from the other two, but the two lowest values become hand to distinguish with in the 100-tip trees.

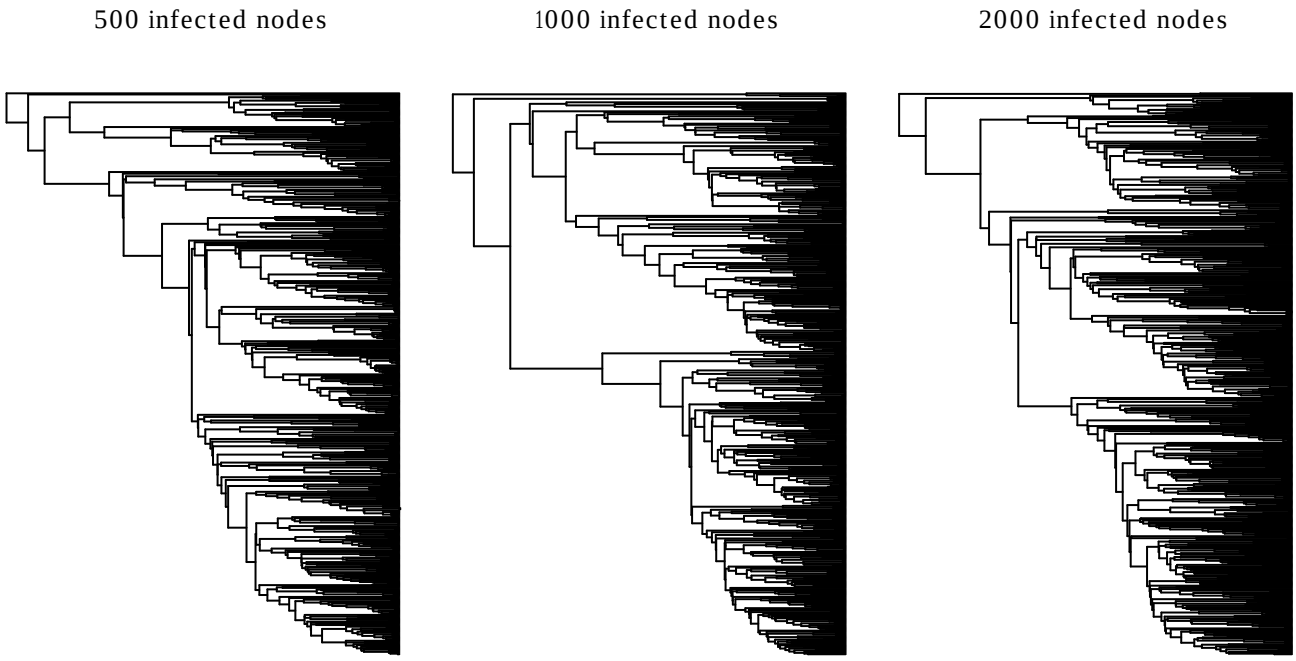

Figure 2.10: Epidemics were simulated on networks of size 5000 until $I = 500$, 1000, or 2000 nodes were infected. When scaled to the same height, there is no immediately visible distinction in shape between trees simulated under different I values.

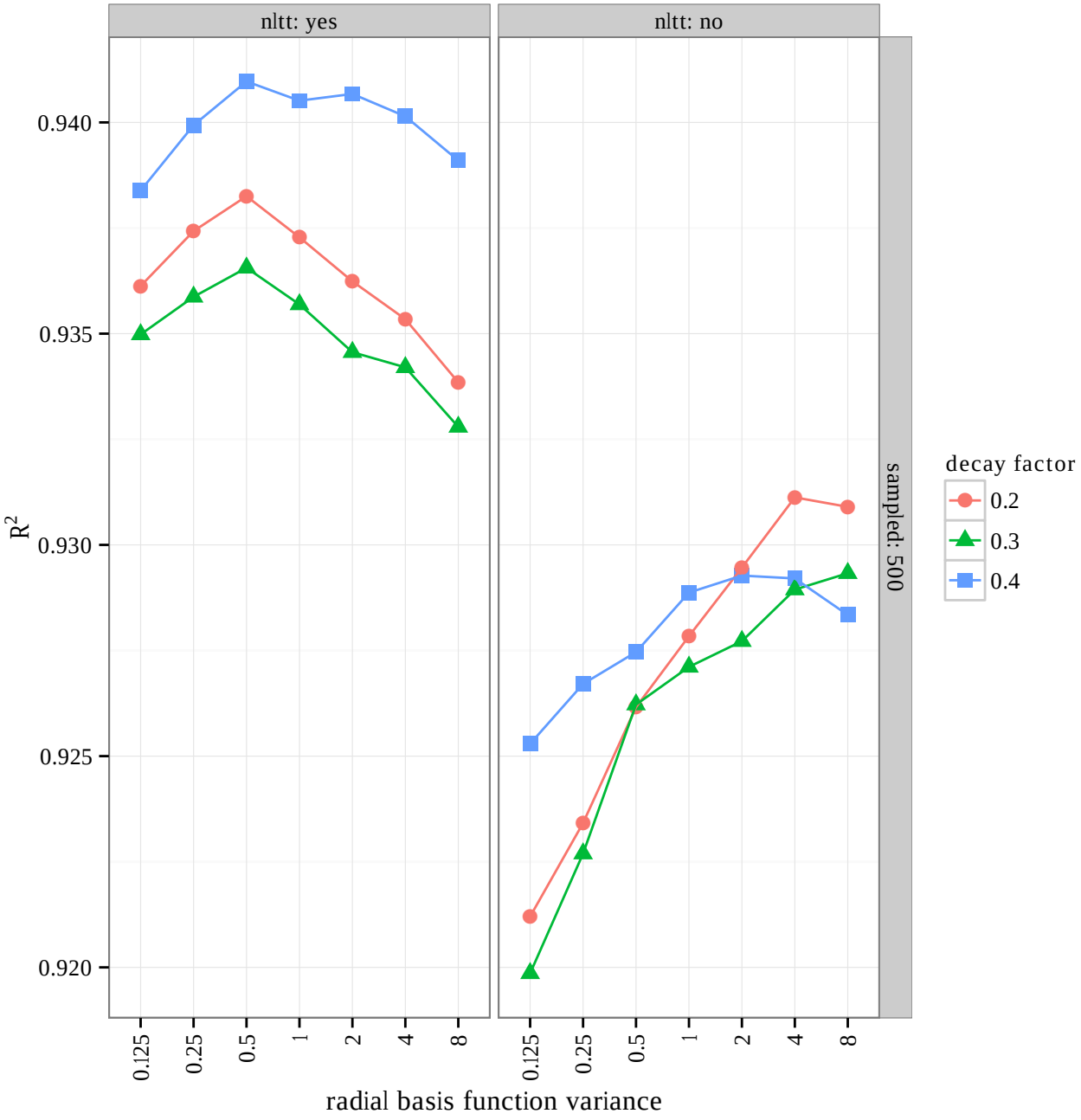

Figure 2.11: For BA networks of size $N = 5000$, a kernel-SVM classifier is very accurate at predicting I. Epidemics were simulated until $I = 500$, 1000, or 2000 nodes were infected, and either 100 or 500 nodes were sampled for inclusion in a transmission tree. The parameters of the BA network were $\alpha = 1.0$ and $m = 2$. A Sackin's index-based classifier performed very poorly on these data (R^2 = TODO for 100-tip trees and blah for 500-tip trees, not shown).

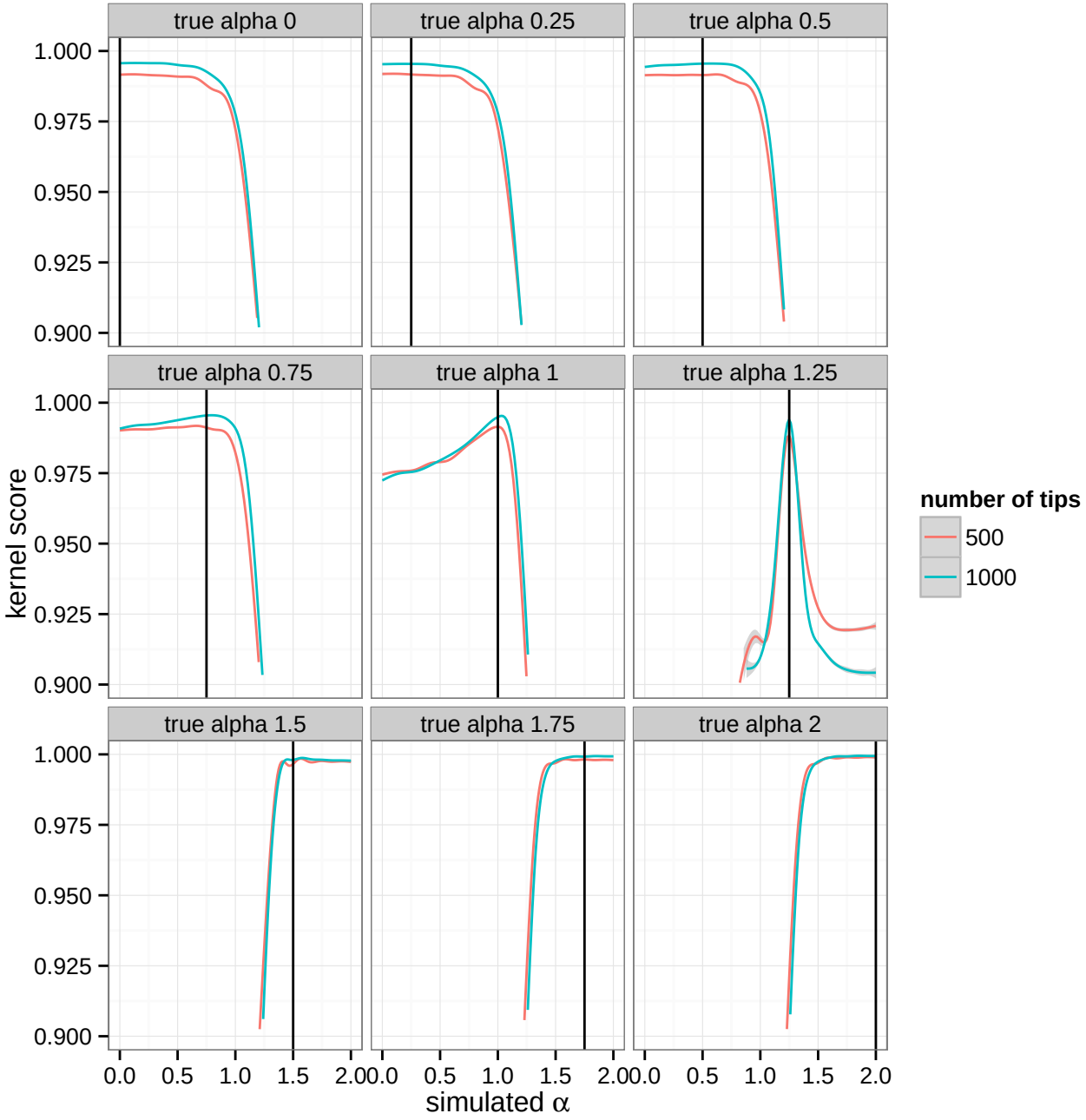

Figure 2.12: Grid search kernel scores for testing trees simulated under various α values. All epidemics had $I = 1000$ infected nodes, on BA networks of size $N = 5000$ with m fixed at 2. Colours indicate the number of sampled tips.

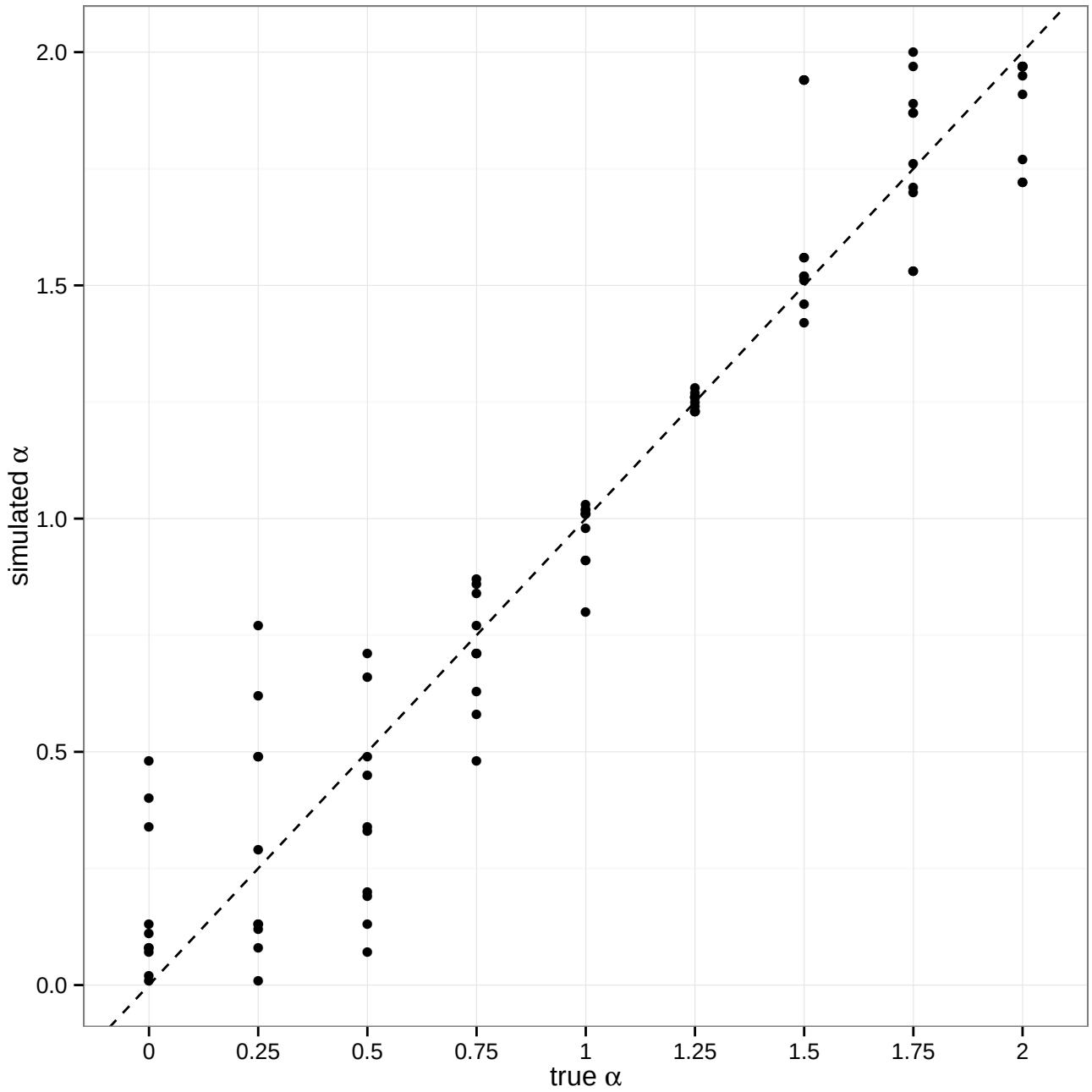

Figure 2.13: Marginal estimates of α obtained with grid search. Training trees were simulated on a narrowly spaced grid of α values, and compared to testing trees using the tree kernel. The α value in the grid with the highest median kernel score was taken as the point estimate for the testing tree. These point estimates are shown as black dots. The dashed line is the identity.

Chapter 3

Conclusion

Bibliography

Barabási, Albert-László and Réka Albert (1999). "Emergence of scaling in random networks". In: *science* 286.5439, pp. 509–512.

Baskins, Doug (2004). *Judy arrays*.

Beaumont, Mark A (2010). "Approximate Bayesian computation in evolution and ecology". In: *Annual review of ecology, evolution, and systematics* 41, pp. 379–406.

Britton, Tom and Philip D O'Neill (2002). "Bayesian inference for stochastic epidemics in populations with random social structure". In: *Scandinavian Journal of Statistics* 29.3, pp. 375–390.

Buneman, Peter (1974). "A note on the metric properties of trees". In: *Journal of Combinatorial Theory, Series B* 17.1, pp. 48–50.

Cavalli-Sforza, Luigi L and Anthony WF Edwards (1967). "Phylogenetic analysis. Models and estimation procedures". In: *American journal of human genetics* 19.3 Pt 1, p. 233.

Cottam, Eleanor M et al. (2008). "Integrating genetic and epidemiological data to determine transmission pathways of foot-and-mouth disease virus". In: *Proceedings of the Royal Society of London B: Biological Sciences* 275.1637, pp. 887–895.

Coyne, Jerry A and H Allen Orr (2004). *Speciation*. Vol. 37. Sinauer Associates Sunderland, MA.

Csardi, Gabor and Tamas Nepusz (2006). "The igraph software package for complex network research". In: *InterJournal, Complex Systems* 1695.5, pp. 1–9.

Del Moral, Pierre, Arnaud Doucet, and Ajay Jasra (2012). "An adaptive sequential Monte Carlo method for approximate Bayesian computation". In: *Statistics and Computing* 22.5, pp. 1009–1020.

Didelot, Xavier, Jennifer Gardy, and Caroline Colijn (2014). "Bayesian inference of infectious disease transmission from whole-genome sequence data". In: *Molecular biology and evolution* 31.7, pp. 1869–1879.

Domingo, Esteban, Julie Sheldon, and Celia Perales (2012). "Viral quasispecies evolution". In: *Microbiology and Molecular Biology Reviews* 76.2, pp. 159–216.

Drummond, Alexei J et al. (2003). "Measurably evolving populations". In: *Trends in Ecology & Evolution* 18.9, pp. 481–488.

Erdős, Paul and Alfred Rényi (1960). "On the evolution of random graphs". In: *Publ. Math. Inst. Hungar. Acad. Sci* 5, pp. 17–61.

Fitzpatrick, Benjamin M, JA Fordyce, and S Gavrilets (2008). "What, if anything, is sympatric speciation?" In: *Journal of evolutionary biology* 21.6, pp. 1452–1459.

Gough, Brian (2009). *GNU scientific library reference manual*. Network Theory Ltd.

Grenfell, Bryan T et al. (2004). "Unifying the epidemiological and evolutionary dynamics of pathogens". In: *science* 303.5656, pp. 327–332.

Groendyke, Chris, David Welch, and David R Hunter (2011). "Bayesian inference for contact networks given epidemic data". In: *Scandinavian Journal of Statistics* 38.3, pp. 600–616.

Haeckel, Ernst Heinrich (1866). *Generelle Morphologie der Organismen*. Vol. 2. Verlag von Georg Reimer.

Harding, EF (1971). "The probabilities of rooted tree-shapes generated by random bifurcation". In: *Advances in Applied Probability*, pp. 44–77.

Holmes, Eddie C et al. (1995). "Revealing the history of infectious disease epidemics through phylogenetic trees". In: *Philosophical Transactions of the Royal Society B: Biological Sciences* 349.1327, pp. 33–40.

Hughes, Gareth J et al. (2009). "Molecular phylodynamics of the heterosexual HIV epidemic in the United Kingdom". In: *PLoS Pathog* 5.9, e1000590.

Janzen, Thijs, Sebastian Höhna, and Rampal S Etienne (2015). "Approximate Bayesian Computation of diversification rates from molecular phylogenies: introducing a new efficient summary statistic, the nLTT". In: *Methods in Ecology and Evolution* 6.5, pp. 566–575.

Jombart, T et al. (2011). "Reconstructing disease outbreaks from genetic data: a graph approach". In: *Heredity* 106.2, pp. 383–390.

Karatzoglou, Alexandros et al. (2004). "kernlab-an S4 package for kernel methods in R". In:

Kendall, David G (1948). "On the generalized" birth-and-death" process". In: *The annals of mathematical statistics*, pp. 1–15.

Kingman, John Frank Charles (1982). "The coalescent". In: *Stochastic processes and their applications* 13.3, pp. 235–248.

Klovdahl, Alden S (1985). "Social networks and the spread of infectious diseases: the AIDS example". In: *Social science & medicine* 21.11, pp. 1203–1216.

Leventhal, Gabriel E et al. (2012). "Inferring epidemic contact structure from phylogenetic trees". In: *PLoS Comput Biol* 8.3, e1002413–e1002413.

Marin, Jean-Michel et al. (2012). "Approximate Bayesian computational methods". In: *Statistics and Computing* 22.6, pp. 1167–1180.

Minin, Vladimir N, Erik W Bloomquist, and Marc A Suchard (2008). "Smooth skyride through a rough skyline: Bayesian coalescent-based inference of population dynamics". In: *Molecular biology and evolution* 25.7, pp. 1459–1471.

Moschitti, Alessandro (2006). "Making Tree Kernels Practical for Natural Language Learning." In: *EACL*. Vol. 113. 120, p. 24.

Nee, Sean, Arne O Mooers, and Paul H Harvey (1992). "Tempo and mode of evolution revealed from molecular phylogenies". In: *Proceedings of the National Academy of Sciences* 89.17, pp. 8322–8326.

Nei, Masatoshi and Sudhir Kumar (2000). *Molecular evolution and phylogenetics*. Oxford University Press.

O'Dea, Eamon B and Claus O Wilke (2010). "Contact heterogeneity and phylodynamics: how contact networks shape parasite evolutionary trees". In: *Interdisciplinary perspectives on infectious diseases* 2011.

Poon, Art FY (2015). "Phylodynamic inference with kernel ABC and its application to HIV epidemiology". In: *Molecular biology and evolution*, msv123.

Poon, Art FY et al. (2013). "Mapping the shapes of phylogenetic trees from human and zoonotic RNA viruses". In: *PLoS ONE* 8.11, e78122.

Pybus, Oliver G and Andrew Rambaut (2009). "Evolutionary analysis of the dynamics of viral infectious disease". In: *Nature Reviews Genetics* 10.8, pp. 540–550.

Robinson, Katy et al. (2013). "How the dynamics and structure of sexual contact networks shape pathogen phylogenies". In: *PLoS computational biology* 9.6, e1003105.

Rubin, Donald B et al. (1984). "Bayesianly justifiable and relevant frequency calculations for the applied statistician". In: *The Annals of Statistics* 12.4, pp. 1151–1172.

Schölkopf, Bernhard, Alexander Smola, and Klaus-Robert Müller (1998). "Nonlinear component analysis as a kernel eigenvalue problem". In: *Neural computation* 10.5, pp. 1299–1319.

Sisson, Scott A, Yanan Fan, and Mark M Tanaka (2007). "Sequential monte carlo without likelihoods". In: *Proceedings of the National Academy of Sciences* 104.6, pp. 1760–1765.

Smola, Alex and Vladimir Vapnik (1997). "Support vector regression machines". In: *Advances in neural information processing systems* 9, pp. 155–161.

Stadler, Tanja et al. (2011). "Estimating the basic reproductive number from viral sequence data". In: *Molecular biology and evolution*, msr217.

Sunnåker, Mikael et al. (2013). "Approximate bayesian computation". In: *PLoS Comput Biol* 9.1, e1002803.

Volz, Erik M, Katia Koelle, and Trevor Bedford (2013). "Viral phylodynamics". In: *PLoS Comput Biol* 9.3, e1002947.

Volz, Erik M, James S Koopman, et al. (2012). “Simple epidemiological dynamics explain phylogenetic clustering of HIV from patients with recent infection”. In: *PLoS Comput Biol* 8.6, e1002552–e1002552.